Nitrate Anion Reduction in Aqueous Perchloric Acid as an Electrochemical Probe of Pt{110} - (1x1) Terrace Sites

Gary A. Attard[1]*, Janaina Souza-Garcia[2], Ricardo Martínez-Hincapié[3] and Juan M. Feliu[3]

[1]Department of Physics, Oliver Lodge Laboratory, University of Liverpool, Oxford St, Liverpool L69 7ZE, UK.

[2]Universidade Federal do ABC, Centro de Ciências Naturais e Humanas, Av. dos Estados, 5001, 09210-580, Santo André-SP, Brazil.

[3]Instituto de Electroquímica, Universidad de Alicante, Apartado 99, E-03080, Alicante, Spain.

* To whom correspondence should be addressed:
e-mail: attard@cardiff.ac.uk

Abstract

The electrochemical reduction of nitrate anions in aqueous 0.1 M perchloric acid has been studied using Pt(S)-[n{110}x{111}] and Pt(S)-[n{110}x{100}] single crystal electrodes. It is demonstrated that the presence of Pt{110} adsorption sites is associated with a single, broad nitrate reduction peak centred at 0.18 V (RHE). Moreover, depending on the cooling environment used after flame-annealing (CO, H_2, Ar, air, nitrogen), the surface concentration of such sites varies which in turn regulates the nitrate reduction current density achievable for a given stepped Pt{hkl} electrode. The origin of this phenomenon is the propensity of the clean Pt{110} basal plane (and vicinal surfaces containing this plane) to reconstruct towards a stable (1x2) phase with strong CO chemisorption favouring formation of larger Pt{110}-(1x1) domains. In contrast, argon/air-cooling appears to promote the development of a largely (1x2) reconstructed surface which is much less active for nitrate reduction since the surface density of Pt{110}-(1x1) terrace sites is significantly diminished. Interestingly, hydrogen-cooling affords nitrate reduction activity intermediate between these two extremes. We suggest that under this particular preparation condition, a partially deconstructed (1x1) phase forms containing the "excess" 50% of surface atoms (originating from the (1x2) phase) sitting proud of the surface in the form of small (1x1) islands, together with residual (1x2) missing row

regions. Hence, after hydrogen cooling, the nominal Pt{110} surface plane is speculated to exhibit a *wider distribution* of *smaller* terrace widths than found with CO cooling together with residual areas of (1x2). The weaker chemisorption of hydrogen apparently limits the size of the Pt{110}-(1x1) domains achievable and consequently, nitrate reduction activity is diminished. Based on these findings, it is proposed that nitrate reduction may be used as a quantitative electrochemical probe of Pt{110}-(1x1) sites at Pt nanoparticles in an analogous fashion to the method of ammonia electrooxidation presently used to quantify the surface abundance of Pt{100} sites.

Keywords: Platinum Surfaces; Electrocatalysis; Nitrate reduction; Structure sensitive reaction.

1. Introduction

Nitrate reduction at metal electrode surfaces has been the subject of intensive research over many years [1-18], due in many respects to its relevance to several topical environmental concerns such as groundwater remediation (denitrification) [19-21], nuclear waste management [22] and food safety [23]. The complexity of this electrochemical reaction is broadly acknowledged [13] and may be ascribed, at its most basic level, to the many oxidation states (+5 to -3) available to nitrogen-containing nitrate reduction reaction intermediates (e.g. NO_2, HNO_2, NO, N_2O, N_2, NH_2OH, NH_3) and their remarkable chemical stability. Hence, in acidic media, many reaction intermediates formed during the reduction pathway from nitrate to ammonium become important as a function of potential, nitrate concentration and pH. Together with numerous linear and branching reaction stages, opportunities for both selectivity and activity variation via the use of electrocatalysts becomes feasible [13]. That the reaction is structure sensitive at platinum electrodes has been long established [10-12]. It is found that in aqueous acidic media free of specifically adsorbing anions, Pt{110} is the most active platinum

surface for nitrate reduction [11, 13]. Taguchi and Feliu [11] studied the kinetics of the reaction on Pt{110} and reported a Tafel slope of 66 mV per decade for the reaction, close enough to 59 mV per decade to propose that the rate determining step (rds) was a pure chemical reaction followed by an electron transfer. Reaction orders of 0 and 1 for nitrate and protons respectively supported the view that protons were involved in the rds together with a saturated coverage of nitrate [11]. As with many studies involving Pt{110} single crystals (including reference [11]), preparation of the well-defined surface was achieved using Clavilier's flame-annealing method [24] with subsequent cooling of the crystal in a hydrogen atmosphere [25]. In two recent publications, it has been shown that such treatment will lead to a Pt{110} surface that is not optimal so far as long range order is concerned [26, 27]. Rather, in order to generate the largest, defect-free Pt{110}-(1x1) planes, it is necessary to cool a flame-annealed Pt{110} electrode in a stream of CO in order to preclude the formation of Pt{110}-(1x2) reconstructed domains which may subsequently result in surface disorder associated with the lifting of the (1x2) phase to the (1x1) phase [26-31]. Because the surface density of platinum atoms in the (1x2) phase is 50% higher than for the (1x1) phase, lifting of the surface reconstruction will result in an excess of Pt{110}-(1x1) islands on-top of the underlying, flat nominal Pt{110}-(1x1) plane [32]. The analogous Pt{100} hex-reconstructed surface, formed when flame-annealed Pt{100} electrodes are cooled in argon or in ultra-high vacuum, gives rise to similar behaviour and deconstructs to leave small, monoatomic high islands of Pt{100}-(1x1) populating the surface [28, 33-35]. In the present study, the issue of the surface structure of Pt{110} and its influence on nitrate reduction in aqueous 0.1 M perchloric acid is addressed. It has already been demonstrated that the oxygen reduction reaction (ORR) is critically dependent on the reconstructive state of Pt{110} [26]. Since nitrate reduction on platinum electrodes has been shown previously to be highly structure sensitive with greatest activity being reported using Pt{110} electrodes [11], it was thought prudent to consider also the impact of the reconstructive

state of this surface on nitrate reaction kinetics. Hence, the present investigation constitutes the second in a series of electrocatalytic studies focussed on Pt{110} and its surface reconstruction.

2. Experimental

The working electrodes were prepared using the method developed by Clavilier [6]. Before each measurement the electrodes were flame annealed and cooled under H_2+Ar atmosphere or CO atmosphere. Then the electrode was protected with a drop of water saturated with the cooling gas before being transferred to the electrochemical cell. The experiments were carried out in a three electrode configuration, at room temperature. The reference electrode was a hydrogen reference electrode (RHE) connected to the cell through a Luggin capillary, while a large platinum wire was used as counter electrode. The solutions were prepared from $HClO_4$ (Merck Suprapur) KNO_3 and ultrapure water (Elga-Vivendi, 18.2 MΩcm). The system was kept free from oxygen with argon (5N, Air Liquide). The experiments were performed with an EG&G PARC 175 signal generator, an eDAQ EA161 potentiostat, and an eDAQ e-corder ED401 recording system. All nitrate reduction CVs presented correspond to the negative-going potential sweep of the cycle.

3. Results and discussion

3.1 Pt{110} reconstructive behaviour as a function of surface preparation

Figure 1 shows the cyclic voltammograms (CVs) of Pt{110} single crystal electrodes in 0.1 M perchloric acid resulting from different cooling regimes after flame-annealing. All of the data are consistent with previous findings [26, 27] and highlight the lability of the Pt{110} surface in relation to the initial preparation conditions. In **figure 1 (a)**, for CO-cooled electrodes, sharp doublet peaks centred at 0.15, 0.20 and 0.27 V demonstrate the sensitivity of the voltammetric response to the crystal preparation procedure (these peaks are largely absent or much attenuated and broadened using other cooling gases). **Figure 1 (b)** highlights the

corresponding changes manifested in the double layer and oxide electrosorption regions of the voltammogram engendered by varying the cooling environment. Here, the most striking aspect of the preparation procedures employed is the one-to-one correspondence between the intensity of the well-defined oxide adsorption peak at 1.01 V and the series of broader oxide electrosorption peaks lying between 0.6 V and 0.9 V. The larger the 1.01 V peak, the smaller are the peaks lying between 0.6 – 0.9 V. This point is also reflected in the magnitudes of the irreversible oxide stripping peaks on the negative potential going sweep. It is noted also that the air-cooled and Ar-cooled samples display almost identical CV responses which indicates closely similar underlying surface structure. The latter CV profiles are closely similar to that of a nitrogen-cooled Pt{110} electrode reported previously in reference [26]. In reference [26], such behaviour was postulated as arising from varying proportions of (1x1) and (1x2) domains being present with peaks between 0.6 and 0.8 V corresponding to electrosorption at less co-ordinated platinum atoms in the reconstructed phase. Based on the intensity of the doublet at 0.27 V ascribable to the presence of good (1x1) long range order [26] together with the magnitude of the 1.01 V terrace oxide peak, the propensity of each gas to propagate long range (1x1) order is found to be:

$$CO >> H_2 > air \sim Ar \sim N_2$$

That there is still a peak at 1.01 V ascribable to oxide electrosorption at Pt{110}-(1x1) sites, even for the air-cooled electrode, supports the notion of a mixed (1x2)/(1x1) phase being formed as noted in [26], i.e. only a partial lifting of the reconstruction results from hydrogen chemisorption. This is not inconsistent with previous work in UHV [36] which confirmed the stability of the (1x2) reconstruction after hydrogen adsorption by LEED. Indeed, the (1x2) reconstruction was also confirmed by Markovic et al. [29, 37] for hydrogen-cooled Pt{110} electrodes using in situ X-ray diffraction. Hence, both LEED and surface-XRD of a Pt{110}

surface prepared with hydrogen should afford a (1x2) superstructure since only a partial lifting of the (1x2) reconstruction is deduced from consideration of the CV response.

On this basis, the minimal residual electrosorption charge in the range 0.2 to 0.3 V for the argon- and air-cooled samples is ascribed to small Pt{110}-(1x1) islands derived from partial lifting of the clean surface reconstruction since this potential also overlaps precisely with the (1x1) doublet peak observed at 0.27 V.

In order to verify both the presence and extent of reconstructed (1x2) surface phase, a second set of CV experiments was undertaken involving post-treatment with CO (**Figure 2**). Hence, any changes caused by dosing CO onto ostensibly reconstructed domains of Pt{110}-(1x2) should result in removal of any features in the voltammogram ascribable to reconstruction. It is noted in this context that Markovic and co-workers using in situ X-ray surface diffraction actually did not observe a lifting of the Pt{110}-(1x2) reconstruction after CO adsorption under electrochemical control [29]. In contrast, Aldaz et al. did note changes to the Pt{110} voltammetric profile after CO adsorption in alkaline aqueous electrolytes [38-40]. Watanabe et al., [31] using in situ STM also recorded that a Pt{110}-(1x1) phase is formed after cooling a flame-annealed Pt{110} electrode in 1% CO / 99% He gas mixture. Hence, in the absence of any electrochemical control, lifting of the Pt{110} – (1x2) by CO in the gas phase is confirmed. In reference [31], subsequent CO adsorption in the electrochemical cell gave rise to the well-known p_1g_1-(2x1) CO adlayer [41] at full CO coverage in which CO molecules are tilted in opposite directions at alternate Pt atoms along the $[1\bar{1}0]$ direction. Unfortunately, explicit formation of the Pt{110}-(1x2) clean surface followed by CO adsorption was not reported in reference [31]. We are unclear as to why the (1x2) reconstruction appears quite stable after CO adsorption in reference [29] (at least at room temperature), in contrast to findings reported in the surface science literature [42-44]. It is noted however, that

in references [44] and [43], so long as the substrate temperature was kept below 240 K, the (1x2) phase was indeed stable and subsequent CO formation led to a c(8x4)-CO phase on top of the underlying reconstructed (1x2) Pt surface. Subsequent warming of this layer to room temperature resulted in a transformation of the c(8x4)-CO phase to a (1x1) phase with a high background intensity using LEED [44]. In what follows, we interpret the changes observed in the voltammetry of argon- and air-cooled Pt{110} as arising from lifting of (1x2) reconstructed domains based on changes observed in voltammetric features previously ascribed to (1x1) and (1x2) surface structures [26].

In **figure 2 (a)**, the formation of electrochemical oxide on a CO-cooled Pt{110} electrode is, as before, signified by a single, intense feature at 1.01 V with an almost negligible oxide adsorption charge contribution at 0.90 V (previously ascribed to low levels of Pt(S)-[n{110}x{111}] surface defects [27]. After electrochemical oxide adsorption, it is observed in **Figure 2 (b)** that both the so-called hydrogen underpotential deposition (Hupd) peaks and the electrosorbed oxide are irreversibly altered. It is seen that the 0.90 V defect feature is hardly impacted at all after electrosorption of oxide compared to in **Figure 2 (a)**. However, the single oxide peak at 1.01 V now bares a shoulder at more negative potentials clearly associated with surface roughening after oxide adsorption/desorption in the first sweep. Broadening and loss of doublet structure in the Hupd region is also consistent with a disordering of the CO-cooled surface after electrochemical oxide adsorption and desorption [26]. However, the key point is that no oxide peaks are observed between 0.6 and 0.9 V after such treatment and therefore, if such peaks are a manifestation of the (1x2) reconstructed phase, then electrosorption of oxide on Pt{110}-(1x1) electrodes does not appear to lead to their formation. This finding is in agreement with previous work by Markovic and co-workers [29]. In **Figure 2 (c)**, a similar set of experiments are performed for the air-cooled Pt{110} electrode. Here, it is clear that a strong attenuation of the 1.01 V peak has been produced (although it is still present as discussed

earlier) with a high intensity of oxide peaks between 0.6 and 0.9 V. The CV in **Figure 2 (c)** is quite stable within the potential range 0.05 to 0.90 V demonstrating that the (1x2) domains should also be stable in agreement with previous studies [28-30, 45, 46]. This is in contrast to the behaviour of the Pt{100}-hex-R0.7° reconstructed phase which is lifted by hydrogen electrosorption [33-35].

The small oxide peak at 0.99 V is at the same potential as the shoulder peak in **Figure 2 (b)** formed after adsorption and desorption of an electrochemical oxide layer on the pristine (1x1) surface. The Hupd region is especially transformed relative to a CO-cooled surface with two peaks at 0.16 and 0.2 V that overlap with a broad feature extending from 0.2 to 0.35 V, the origins of which have been discussed previously as arising from residual islands of Pt{110}-(1x1).

When the electrode prepared via air-cooling in **Figure 2 (c)** is treated by 10 potential cycles between 0.06 and 0.80 V in an electrolyte saturated with CO, the CV profile in **Figure 2** (d) results. Changes facilitated by this treatment in both the Hupd and oxide potential regions are remarkable. For example, the Hupd region now resembles strongly that obtained via hydrogen cooling (see **Figure 1**) with much more charge density observed between 0.2 and 0.3 V and a loss in intensity of the peaks at 0.2 V. Moreover, the oxide peaks at 0.77 V and 0.82 V are completely attenuated with a corresponding increase in the intensity of the 1.01 V oxide terrace peak. This behaviour is entirely consistent with a model in which lifting of pre-existing (1x2) surface domains to a (1x1) phase by CO chemisorption is afforded but with Pt{110}-(1x1) terraces separated by defects, consistent with small (1x1) islands sitting atop the Pt{110} plane as discussed earlier. The defect sites formed after CO adsorption/desorption give rise to peaks at 0.86 and 0.91 V. If this is indeed the case, such an interpretation positively identifies peaks at 0.78 and 0.82 V as arising from oxide adsorption on sites present within the Pt{110}-(1x2) reconstruction as speculated previously in [26]. In Table S1, we list the positions of

terrace and step oxide peak potentials for Pt{hkl}. It is evident from Table S1 that a simple relationship pertains, i.e. the potential at which oxide formation occurs reflects the atomic coordination of atoms within the surface site. Those sites associated with highly coordinated terrace sites are oxidised at potentials more positive than the less coordinated step sites. It is noted however that the peaks at 0.82 and 0.78 V are at more negative potentials than oxide adsorption peaks arising even from linear steps. This low oxidation potential we associate with a high degree of oxyphilicity caused by highly unsaturated atoms in the (1x2) "rails" of Pt atoms along the $[1\bar{1}0]$ direction [26]. Atoms at the ends of these chains should provide an even more oxyphilic environment because they afford an even lower degree of surface coordination. Hence, we ascribe the peaks at 0.82 V and 0.78 V to oxide adsorption at sites in the "rails" of the Pt(110)-(1x2) surface reconstruction and defects (such as generated by vacancies) within these rails respectively. It is predicted that isolated atoms not belonging to "rail" structures should exhibit the lowest oxide potentials of all. In order to identify the origin of the 0.2 V peak observed for air-cooled Pt{110}, comparison is made with the CV of Pt{331} which displays the narrowest average {110} terrace width (n = 2) and also gives rise to a peak close to 0.2 V (figure SI 1). Although not an exact match of potentials, it is reported that this peak shifts to slightly more positive potentials for n > 2 [10, 47]. In reference [47], the 0.2 V peak was ascribed to variations in the magnitude of two dimensional Pt{110} long range order. We agree with this interpretation and ascribe the 0.2 V peak to electrosorption on very narrow Pt{110} terraces or as a corollary, a highly disordered Pt{110}-(1x1) phase. It is interesting in this context that recent work from the Koper group [48] has identified the so-called "third peak" observed in the Hupd region of Pt as arising from single atoms adding to/moving away from sites at the end of such Pt{110}-type "rails". The potential of the "third peak" is precisely at 0.2 V but is only generated after excursions into the hydrogen evolution reaction potential range. In **figure 3**, we show the result of this treatment on Pt{110} prepared using different

cooling ambients. The results for **figure 3 (b)** has already been reported [49] whereby hydrogen cooled Pt{110} generates a "third peak" feature of significant intensity. It is evident that air-cooled Pt{110} also gives rise to this feature to a similar degree. Astonishingly, for a CO-cooled Pt{110} electrode, the magnitude of the "third peak" is negligible in comparison (**figure 3 (c**)). We conclude from this measurement that a combination of Pt{110} symmetry and significant surface disorder is required to generate the so-called "third peak". If the origin of this feature is as described recently by Koper et al [48], to movement of Pt atoms at the ends of 110 chains, it means that such sites are largely absent in CO-cooled Pt{110} electrodes attesting once again to the high degree of long range surface order. Returning to **Figure 1 (b)**, for the hydrogen cooled electrode, it is clear that the oxide region consists of peaks at 0.81, 0.91, 0.99 and 1.01 V. The peak at 0.81 V provides implicit indications for some residual (1x2) being present even for hydrogen-cooled Pt{110} electrodes although the latter three peaks are consistent with a *wider distribution* of *smaller* terrace widths than found with CO cooling (also consistent with generation of "third peak" features), which also manifests itself as a rather broad Hupd region centred at 0.23 V. It is proposed that the weaker chemisorption of hydrogen compared to CO apparently limits the size of the Pt{110}-(1x1) domains obtainable. It is also interesting to consider the fact that oxygen exhibits a greater magnitude of enthalpy of adsorption than CO on Pt [50]. Hence, one would predict that cooling in air might lead to complete lifting of the (1x2) reconstruction if chemisorption strength was the sole arbiter of (1x2) stability. However, one must also remember that the sticking probability of oxygen on the Pt{110}-(1x2) surface is very low, much lower than for CO and this fact can lead to interesting spatio-temporal oscillations in CO surface oxidation kinetics at Pt{110} [51-53]. Therefore, we assert that because of the low sticking for dissociative adsorption of oxygen on Pt{110}-(1x2) in air compared to CO, it fails to lift the surface reconstruction fully (unlike CO which exhibits a high sticking probability to Pt{110}-(1x2) and a reasonably high adsorption

enthalpy, sufficient to de-stabilise (1x2) relative to (1x1)). The residual (1x1) domains left after Ar- and air-cooling are probably the result of a small amount of residual oxygen dissociative chemisorption so their elimination should afford a "perfect" Pt{110}-(1x2). **Figure SI 2** shows a compilation of data from **figure 2** in a single figure emphasising the obvious changes occurring upon CO adsorption/electrochemical oxidation.

Inspection of Table S1 shows also that the oxide peaks at 0.84, 0.91 and 0.99 V are consistent with the presence of Pt(S)-[n{100}x{110}], Pt(S)-[n{110}x{111}] and Pt(S)-[n{111}x{111}] linear step sites respectively and all of these sites should be present in the step edges of small monoatomic and multilayer islands of Pt{110}-(1x1) sitting proud of the Pt{110} plane. In **figure SI 3**, hard sphere models of these structures are shown and the various step sites highlighted.

Finally, in this section we report CO-charge displacement measurements of potential of zero total charge (PZTC) [27, 47, 49] for CO-, hydrogen- and air cooled Pt{110} (**Figure 4**).

The shift of PZTC from 0.245 V (CO-cooled) to 0.210 V (air-cooled) is consistent with a gradual diminution in the mainly "anionic" charge associated with the electrosorption peak centred at 0.27 V corresponding to "OH" adsorption on long range ordered Pt{110}-(1x1) domains [27]. The total integrated charge measured from 0.05 to 0.4 V is closely similar for all surfaces studied although the individual "cationic" and "anionic" charge contributions do vary, again ascribable largely to changes in the magnitude of the voltammetric peak at 0.27 V. As mentioned in previous studies [29, 30, 38 - 40, 42, 43], it is curious that given the profound changes in surface structure taking place with different cooling methods that the so-called "hydrogen underpotential deposition charge" (H upd) remains relatively constant. Previous interpretations of this phenomenon have speculated upon the number of hydrogen atoms adsorbed per surface unit cell for the (1x1) and (1x2) surfaces [28, 29]. The only comment we

wish to make in this context is that at least for the CO-cooled surface, a complex co-adsorption of cationic and anionic species pertains over this potential range [27] and that ascribing even the majority of "Hupd charge" solely to "hydrogen" is probably not correct. Rather, it is more likely that differing amounts and ratios of anionic to cationic species adsorb/desorb as a function of potential depending on the overall surface structure govern the Hupd charge one obtains. Hence, a strict one-to-one correspondence between the surface density of Pt atoms and the number of electrons transferred per Pt atom is probably an approximation.

3.2 The reconstructive state of Pt(S)-[n{110}x{111}] and Pt(S)-[n{110}x{100}] electrodes and electrocatalytic activity towards nitrate reduction

In **figure 5** is shown the data obtained for nitrate reduction in 0.1 M aqueous perchloric acid using Pt(S)-[n{110}x{111}] and Pt(S)-[n{110}x{100}] electrodes.

It is noted that a single reduction peak centred at 0.18 V results for all systems studied, irrespective of cooling conditions after flame-annealing. We also include in **Figure SI 4** nitrate reduction CVs for hydrogen-cooled Pt{111}, Pt{100}, Pt{311}, Pt{331}, Pt{210} and Pt{110} demonstrating negligible nitrate reduction activity at 0.18 V for platinum electrodes not containing {110} sites.

It is observed that for a given stepped Pt{110} electrode, the nitrate reduction current obtained is greatest for CO-cooled surfaces, lowest for air-cooled surfaces and intermediate for hydrogen cooled electrodes. This trend is precisely that observed for Pt{110} electrodes if it is assumed that varying degrees of long range Pt{110}-(1x1) order are regulating the magnitude of the nitrate reduction current. Furthermore, since the introduction of more and more linear steps into the surface of Pt{110}, by definition, should lead to a decrease in the population of Pt{110}-(1x1) sites available, nitrate reduction activity should decrease. This is evidently the case since, irrespective of cooling conditions, a surface containing more steps exhibits a lower

activity than a less stepped surface. A plot of nitrate reduction current density versus step density is given in **figure 6** in order to assess if there is a *direct* relationship between these two parameters. It clear from **Figure 6** that for Pt(S)-[n{110}x{111}] electrodes cooled in CO, there is a linear relationship and therefore it is asserted that the site of greatest activity for nitrate reduction is Pt{110}-(1x1). The corresponding hydrogen-cooled electrodes also give rise to a linear dependency of nitrate reduction current density versus step density but with a shallower gradient than for the CO data. We interpret this finding as a consequence of the intrinsically more disordered nature of the hydrogen-cooled surfaces compared to the CO-cooled electrodes and this impact on the quality of the Pt{110}-(1x1) terraces scales linearly with step density since this in turn determines how many Pt{110}-(1x1) sites are present. Pt{331} is the turning point of the zone and may be written Pt(S)-2{110}x{111} and the intrinsic nitrate activity of this highly stepped surface is asserted to arise from the Pt{110} part of the step. It is predicted therefore, that defects introduced into such a step (such as kinks) should lead to a further decrease in nitrate reduction current density because they decrease {110} symmetric sites. In order to explain the results for Pt(S)-[n{110}x{111}] surfaces cooled in air, which all exhibit nitrate reduction current density values smaller than Pt{331}, one has to assert that the availability of Pt{110}-(1x1) sites must be still more limited. In fact, this would be completely consistent with an interpretation in which all air-cooled Pt(S)-[n{110}x{111}] electrodes are reconstructed such that the majority of Pt{110}-(1x1) sites (steps and terraces) are removed. The obvious mechanism for interpreting this is a switch from (1x1)- to (1x2)-dominated, reconstructed domains for the Pt{110} parts of the terrace. It is difficult to expand further on the fate of the linear steps (whether they are incorporated into the surface reconstruction itself or remain unperturbed) but there is no doubt that removal of Pt{110}-(1x1) sites diminishes nitrate reduction activity at platinum. For air-cooled Pt{331}, since only a very small nitrate reduction current density is observed compared to CO-cooled

analogues, it is evident that even the Pt{110} part of the step is utterly disrupted such that little linear Pt{110}x{111} step character remains.

Hence, if the magnitude of the nitrate reduction current is a manifestion of the surface density of Pt{110}-(1x1) sites then one may use **Figure 6** to estimate what this percentage might be assuming that a CO-cooled Pt{110} electrode is comprised of 100% of such sites (ignoring the very small number of defects associated with oxide adsorption at 0.91 V in **figure 1**). Based on this hypothesis, we assert that to a first approximation, the surface percentage of Pt{110}-(1x1) sites present (including steps and terraces) is given by:

Nitrate peak reduction current density / Nitrate peak reduction current density for CO-cooled Pt{110}…. (1)

Hence, for the hydrogen-cooled Pt{110} electrode, a value of approximately 55% is obtained using equation 1 with the residual 45% of surface sites corresponding to all other possible sites. Since other Pt{hkl} sites also give rise to some residual nitrate reduction current density at 0.18 V (see **Figure SI 4**) of at most 35 μA per cm^2, a small uncertainty needs to be placed on this evaluation of at most 3%. It is interesting that good agreement of this determination and a value of 50% Pt{110}-(1x1) sites estimated for a hydrogen-cooled Pt{110} surface in reference [47] using a different method to that used here is achieved.

Nonetheless, the linear dependence of nitrate reduction current density on step density for CO-cooled (and hence, unreconstructed Pt(S)-[n{110}x{111}] surfaces [26, 27] affords a direct interpretation and quantification of Pt{110}-(1x1) sites present.

When extended to air-cooled samples, the prediction of 4 -18% Pt{110}-(1x1) sites depending on Pt{hkl} gives the order of magnitude change in surface order facilitated by such treatment. The method proposed here to quantify the surface concentration of Pt{110}-(1x1) sites should also be applicable to any platinum surface (including Pt nanoparticles) in a similar

fashion to the method of ammonia oxidation, presently used to quantify the surface concentration of Pt{100} sites [54-56].

We now examine the raw data for nitrate reduction using Pt(S)-[n{110}x{100}] electrodes in **figure 4** as a function of cooling gas after flame-annealing and replot the peak reduction current density as a function of step density (**Figure 7**).

It was noted already in reference [27] that the introduction of "{100}" steps into the Pt{110} plane created an unstable situation whereby the step sites reconstructed to give rise to a facetted, stepped Pt{110} surface with significantly reduced Pt{110}-(1x1) long range order, even for CO-cooled samples. This was especially true for $n \geq 4$ as reflected in the magnitude of the 1.01 V oxide peak and a general diminution and broadening of all Pt{110}-(1x1) electrosorption sites compared with when "{111}" steps were incorporated into the basal Pt{110} plane at a similar surface density. Hence, it is not surprising to see this phenomenon reflected in the nitrate reduction current density data reported in **figure 7**. For example, although the hydrogen-cooled Pt(S)-[n{110}x{100}] electrodes give rise to a linear decrease in nitrate activity as a function of step density (as also seen in **Figure 6**), it is evident that a non-linear monotonic decrease is observed for the CO-cooled surfaces. In fact, both hydrogen- and CO-cooled curves overlap for narrow terraces ($n \leq 4$). Clearly within the model expounded in the present study, overlap of nitrate reduction data points, irrespective of hydrogen- or CO-cooling suggests similar surface densities of Pt{110}-(1x1) sites. In fact, in **Figure SI** 5 is shown the CV data for CO- and hydrogen-cooled Pt{430} and Pt{210} displaying very similar CV profiles in comparison to the less stepped Pt{20, 19, 0} and Pt{10, 9, 0} surfaces.

For wider terraces ($n > 4$), CO-cooled samples evidently support a greater degree of Pt{110}-(1x1) order relative to their hydrogen-cooled analogues. That there is not a smooth, linear relationship going from CO-cooled Pt{110} to CO-cooled Pt{210} would be consistent

with surface faceting leading to a reduced value of terrace width compared to that predicted by a simple hard sphere model of a stepped (1x1) surface. Therefore, we assert that, based on nitrate reduction current density measurements as a function of step density, for Pt(S)-[n{110}x{100}] stepped surfaces, the very open step structure reconstructs such that the nominal, average Pt{110} terrace width is diminished. This effect is so strong that for terraces in which $n \leq 4$, even CO-cooling cannot overcome the tendency to facet. Moreover, because there is hardly any difference in CO- and hydrogen- cooled CV behaviour for these narrow terraces, it may even be that they do not exhibit a defect-free (1x1) at all and both correspond to surfaces containing negligible Pt{110}-(1x1) terrace and step sites.

We suggest that the products formed from nitrate reduction are essentially the same as those previously reported [5, 8, 10, 12] including NO(ad) and ammonium cations. It should be noted that in the present study, the whole of the reduction current has been assigned to nitrate reduction rather than NO(ad) which is also redox active in this potential range [57]. Although we have not explicitly investigated the mechanism of nitrate reduction in this study, two issues indicate to us that nitrate reduction belongs to a class of redox reaction which also includes nitrous oxide reduction, persulphate reduction and nitrite reduction, that reflect i) a weakly adsorbed reactant relative to other double layer species (hydrogen underpotential deposition (Hupd) species / anion adsorption / water dipoles) and ii) also give rise to a peak maxima close to the local pzc of the electrode surface [57-62]. In this way, the decomposition mechanism of nitrate is assumed to follow closely that which was outlined previously by Attard and co-workers in the case of nitrous oxide reduction [63] and indeed Koper et al. for nitrate reduction [12]. The sequential loss of each oxygen atom via N-O bond dissociation until NO(ad) remains [8] is predicated on the initial adsorption of nitrate at “free” metal sites. Hence, the reduction current observed is essentially a reflection of the free metal sites available to the nitrate anion as a function of potential, not the amount of pre-existing NO(ad) which also is redox active in

this potential range. NO(ad) would act as a blocking agent if formed (and would also lift the (1x2) reconstruction at sufficiently high coverages [64]) and so one might expect some hysteresis in the nitrate reduction current on forward and reverse potential sweeps since NO(ad) is removed at negative potentials [12, 57]. This would only be a minor contribution based on the magnitude of NO(ad) stripping currents observed at high NO(ad) coverage [12, 57] and at highly defective Pt{hkl} surfaces which exhibit the same "bell-shaped" reduction curve as well-ordered Pt{110}-(1x1) electrodes rather than discrete and narrow stripping peaks when present at saturation coverage [12, 57]. Hence, NO(ad) may indeed be being formed as a reaction intermediate during this process. However, the magnitude and peak width of the nitrate reduction peak is not consistent with NO reduction alone [12, 57]. Rather, the major factor determining the magnitude of the nitrate reduction current is fast decomposition of electrosorbed nitrate. Within this model, it may not necessarily be the local atomic structure of Pt{hkl} either that determines nitrate reduction activity but rather the extent of "blocking" by double layer components such as monopoles and dipoles as a function of potential. The high electrocatalytic activity of terrace sites is not unprecedented. There are already a number of examples reported in the literature of the high electrocatalytic activity exhibited by terraces including for ammonia oxidation at Pt{100} [54 - 55], nitrite reduction [61] and oxygen reduction in alkali at Pt{111} [65]. We speculate that the reason for the high activity of Pt{110}-(1x1) towards nitrate reduction stems from the inherently weak adsorption of nitrate at Pt{hkl} coupled with the competitive adsorption of dipoles and monopoles as a function of potential. The relative inactivity of defect sites would then correspond to even weaker competitive adsorption due to site blocking by these same double layer components that are presumably more strongly bound to defect sites than terraces, especially around the local pzc.

4. Conclusion

An extensive investigation of different flame-annealing and cooling protocols has been undertaken using Pt(S)-[nPt{110}x{111}] and Pt(S)-[nPt{110}x{100}] stepped single crystal electrodes in order to elucidate the role of surface reconstruction in influencing the surface sensitive nitrate reduction reaction. Based on considerations of voltammetric features associated with Hupd and oxide formation both before and after CO dosing and stripping, it is concluded that nitrate reduction current density is highly sensitive to the degree of Pt{110}-(1x1) long range order. Moreover, based on quantitative relationships between the nitrate reduction current density and step density, it is proposed that nitrate reduction may be used as a probe of Pt{110}-(1x1) sites in an analogous fashion to the method of ammonia oxidation presently utilised in Pt{100} site determination [54-56]. In addition, it is asserted that in contrast to CO-cooled Pt{110} electrodes which give rise to an exclusively (1x1) surface (after CO is removed), hydrogen- and air-cooled surfaces give rise to only a partial lifting of the clean surface (1x2) reconstructed phase. The ratio of (1x1) to (1x2) domains is greatest for hydrogen-cooled samples and this mixture of reconstructed and deconstructed regions is proposed to account for the rather broad Hupd feature of the voltammogram centred at 0.25 V seen with hydrogen – cooled Pt{110} substrates.

Acknowledgements

This study was financed in part by the Coordenação de Aperfeiçoamento de Pessoal de Nível Superior - Brasil (CAPES) - Finance Code 001. JMF wishes to thank MINECO for support from project CTQ2016-76221-P(AEI/FEDER,UE).

References

[1] M.C. Figueiredo, J. Souza-Garcia, V. Climent, J.M. Feliu, Nitrate reduction on Pt(1 1 1) surfaces modified by Bi adatoms, Electrochemistry Communications, 11 (2009) 1760-1763.
[2] M.C. Figueiredo, F.J. Vidal-Iglesias, J. Solla-Gullón, V. Climent, J.M. Feliu, Nitrate reduction on platinum (111) surfaces modified with Bi: Single crystals and nanoparticles, Zeitschrift fur Physikalische Chemie, 226 (2012) 901-917.
[3] M.C. Figueiredo, J. Solla-Gullón, F.J. Vidal-Iglesias, V. Climent, J.M. Feliu, Nitrate reduction at Pt(1 0 0) single crystals and preferentially oriented nanoparticles in neutral media, Catalysis Today, 202 (2013) 2-11.

[4] E.B. Molodkina, M.R. Ehrenburg, Y.M. Polukarov, A.I. Danilov, J. Souza-Garcia, J.M. Feliu, Electroreduction of nitrate ions on Pt(1 1 1) electrodes modified by copper adatoms, Electrochimica Acta, 56 (2010) 154-165.
[5] E.B. Molodkina, I.G. Botryakova, A.I. Danilov, J. Souza-Garcia, J.M. Feliu, Mechanism of nitrate electroreduction on Pt(100), Russian Journal of Electrochemistry, 48 (2012) 302-305.
[6] E.B. Molodkina, I.G. Botryakova, A.I. Danilov, J. Souza-Garcia, J.M. Feliu, Kinetics and mechanism of nitrate and nitrite electroreduction on Pt(100) electrodes modified by copper adatoms, Russian Journal of Electrochemistry, 49 (2013) 285-293.
[7] E.B. Molodkina, A.I. Danilov, M.R. Ehrenburg, J.M. Feliu, Regularities of nitrate electroreduction on Pt(S)[n(100)x(110)] stepped platinum single crystals modified by copper adatoms, Electrochimica Acta, 278 (2018) 165-175.
[8] J. Souza-Garcia, E.A. Ticianelli, V. Climent, J.M. Feliu, Nitrate reduction on Pt single crystals with Pd multilayer, Electrochimica Acta, 54 (2009) 2094-2101.
[9] J. Souza-Garcia, E.A. Ticianelli, V. Climent, J.M. Feliu, Mechanistic changes observed in heavy water for nitrate reduction reaction on palladium-modified Pt(hkl) electrodes, Chemical Science, 3 (2012) 3063-3070.
[10] S. Taguchi, J.M. Feliu, Electrochemical reduction of nitrate on Pt(S)[n(1 1 1) × (1 1 1)] electrodes in perchloric acid solution, Electrochimica Acta, 52 (2007) 6023-6033.
[11] S. Taguchi, J.M. Feliu, Kinetic study of nitrate reduction on Pt(1 1 0) electrode in perchloric acid solution, Electrochimica Acta, 53 (2008) 3626-3634.
[12] G.E. Dima, G.L. Beltramo, M.T.M. Koper, Nitrate reduction on single-crystal platinum electrodes, Electrochimica Acta, 50 (2005) 4318-4326.
[13] V. Rosca, M. Duca, M.T. DeGroot, M.T.M. Koper, Nitrogen Cycle Electrocatalysis, Chemical Reviews, 109 (2009) 2209-2244.
[14] J. Yang, F. Calle-Vallejo, M. Duca, M.T.M. Koper, Electrocatalytic reduction of nitrate on a Pt electrode modified by p-block metal adatoms in acid solution, ChemCatChem, 5 (2013) 1773-1783.
[15] Y.Y. Birdja, J. Yang, M.T.M. Koper, Electrocatalytic reduction of nitrate on tin-modified palladium electrodes, Electrochimica Acta, 140 (2014) 518-524.
[16] J. Yang, P. Sebastian, M. Duca, T. Hoogenboom, M.T.M. Koper, PH dependence of the electroreduction of nitrate on Rh and Pt polycrystalline electrodes, Chemical Communications, 50 (2014) 2148-2151.
[17] J. Shen, Y.Y. Birdja, M.T.M. Koper, Electrocatalytic Nitrate Reduction by a Cobalt Protoporphyrin Immobilized on a Pyrolytic Graphite Electrode, Langmuir, 31 (2015) 8495-8501.
[18] E. Pérez-Gallent, M.C. Figueiredo, I. Katsounaros, M.T.M. Koper, Electrocatalytic reduction of Nitrate on Copper single crystals in acidic and alkaline solutions, Electrochimica Acta, 227 (2017) 77-84.
[19] S. Garcia-Segura, M. Lanzarini-Lopes, K. Hristovski, P. Westerhoff, Electrocatalytic reduction of nitrate: Fundamentals to full-scale water treatment applications, Applied Catalysis B: Environmental, 236 (2018) 546-568.
[20] A. Menció, J. Mas-Pla, N. Otero, O. Regàs, M. Boy-Roura, R. Puig, J. Bach, C. Domènech, M. Zamorano, D. Brusi, A. Folch, Nitrate pollution of groundwater; all right…, but nothing else?, Science of The Total Environment, 539 (2016) 241-251.
[21] A. Kapoor, T. Viraraghavan, Nitrate Removal From Drinking Water—Review, Journal of Environmental Engineering, 123 (1997) 371-380.
[22] J.D. Genders, D. Hartsough, D.T. Hobbs, Electrochemical reduction of nitrates and nitrites in alkaline nuclear waste solutions, Journal of Applied Electrochemistry, 26 (1996) 1-9.
[23] J.J. Sindelar, A.L. Milkowski, Human safety controversies surrounding nitrate and nitrite in the diet, Nitric Oxide, 26 (2012) 259-266.
[24] J. Clavilier, R. Faure, G. Guinet, R. Durand, Preparation of monocrystalline Pt microelectrodes and electrochemical study of the plane surfaces cut in the direction of the {111} and {110} planes, Journal of Electroanalytical Chemistry and Interfacial Electrochemistry, 107 (1980) 205-209.

[25] J. Clavilier, K. El Achi, A. Rodes, In situ probing of step and terrace sites on Pt(S)-[n(111) × (111)] electrodes, Chemical Physics, 141 (1990) 1-14.
[26] G.A. Attard, A. Brew, Cyclic voltammetry and oxygen reduction activity of the Pt{110}-(1×1) surface, Journal of Electroanalytical Chemistry, 747 (2015) 123-129.
[27] G.A. Attard, K. Hunter, E. Wright, J. Sharman, R. Martínez-Hincapié, J.M. Feliu, The voltammetry of surfaces vicinal to Pt{110}: Structural complexity simplified by CO cooling, Journal of Electroanalytical Chemistry, 793 (2017) 137-146.
[28] L.A. Kibler, A. Cuesta, M. Kleinert, D.M. Kolb, In-situ STM characterisation of the surface morphology of platinum single crystal electrodes as a function of their preparation, Journal of Electroanalytical Chemistry, 484 (2000) 73-82.
[29] N.M. Marković, B.N. Grgur, C.A. Lucas, P.N. Ross, Surface electrochemistry of CO on Pt(110)-(1 × 2) and Pt(110)-(1 × 1) surfaces, Surface Science, 384 (1997) L805-L814.
[30] R. Michaelis, D.M. Kolb, Stability and electrochemical properties of reconstructed Pt(110), Journal of Electroanalytical Chemistry, 328 (1992) 341-348.
[31] M. Wakisaka, S. Asizawa, T. Yoneyama, H. Uchida, M. Watanabe, In Situ STM Observation of the CO Adlayer on a Pt(110) Electrode in 0.1 M HClO4 Solution, Langmuir, 26 (2010) 9191-9194.
[32] G. Beitel, O.M. Magnussen, R.J. Behm, Atomic structure of clean and Cu covered Pt(110) electrodes, Surface Science, 336 (1995) 19-26.
[33] A. Al-Akl, G.A. Attard, R. Price, B. Timothy, Voltammetric and UHV characterisation of the (1 × 1) and reconstructed hex-R0.7° phases of Pt{100}, Journal of Electroanalytical Chemistry, 467 (1999) 60-66.
[34] A. Al-Akl, G. Attard, R. Price, B. Timothy, Comparison between gas-phase and electrochemical deposition of copper on Pt(100)-(1 × 1) and Pt(100)-hex-R0.7°, Journal of the Chemical Society, Faraday Transactions, 91 (1995) 3585-3591.
[35] M. Wakisaka, M. Sugimasa, J. Inukai, K. Itaya, Structural Change and Electrochemical Behavior of Pt(100)-hex-R0.7° Surfaces in Gases and in Solution, Journal of The Electrochemical Society, 150 (2003) E81-E88.
[36] J.R. Engstrom, W. Tsai, W.H. Weinberg, The chemisorption of hydrogen on the (111) and (110)-(1×2) surfaces of iridium and platinum, The Journal of Chemical Physics, 87 (1987) 3104-3119.
[37] C.A. Lucas, N.M. Marković, P.N. Ross, Surface Structure and Relaxation at the Pt(110)/Electrolyte Interface, Physical Review Letters, 77 (1996) 4922-4925.
[38] E. Morallón, J.L. Vázquez, A. Aldaz, Electrochemical behaviour of basal single crystal Pt electrodes in alkaline medium, Journal of Electroanalytical Chemistry and Interfacial Electrochemistry, 288 (1990) 217-228.
[39] E. Morallón, J.L. Vázquez, A. Aldaz, J. Clavilier, Electrochemical behaviour of Pt(110) in carbonate and bicarbonate solutions, Journal of Electroanalytical Chemistry and Interfacial Electrochemistry, 316 (1991) 263-274.
[40] E. Morallón, J. Vázquez, R. Duo, A. Aldaz, Electrochemical studies of adsorbed CO on Pt(110) in a carbonate solution: structural surface modification, Surface Science, 265 (1992) 95-101.
[41] S.R. Bare, P. Hofmann, D.A. King, Vibrational studies of the surface phases of CO on Pt{110} at 300 K, Surface Science, 144 (1984) 347-369.
[42] C.M. Comrie, R.M. Lambert, Chemisorption and surface structural chemistry of carbon monoxide on Pt(110), Journal of the Chemical Society, Faraday Transactions 1: Physical Chemistry in Condensed Phases, 72 (1976) 1659-1669.
[43] T.E. Jackman, J.A. Davies, D.P. Jackson, P.R. Norton, W.N. Unertl, A new surface phase for CO-covered Pt(110), Journal of Physics C: Solid State Physics, 15 (1982) L99-L104.
[44] S. Ferrer, H.P. Bonzel, The preparation, thermal stability and adsorption characteristics of the non-reconstructed Pt(110)−1 × 1 surface, Surface Science, 119 (1982) 234-250.
[45] E. Yeager, A. Homa, B.D. Cahan, D. Scherson, Spectroscopic techniques for the study of solid–liquid interfaces, Journal of Vacuum Science and Technology, 20 (1982) 628-633.

[46] A.S. Homa, E. Yeager, B.D. Cahan, Leed-aes thin-layer electrochemical studies of hydrogen adsorption on platinum single crystals, Journal of Electroanalytical Chemistry and Interfacial Electrochemistry, 150 (1983) 181-192.
[47] J. Souza-Garcia, V. Climent, J.M. Feliu, Voltammetric characterization of stepped platinum single crystal surfaces vicinal to the (1 1 0) pole, Electrochemistry Communications, 11 (2009) 1515-1518.
[48] O. Diaz-Morales, T.J.P. Hersbach, C. Badan, A.C. Garcia, M.T.M. Koper, Hydrogen adsorption on nano-structured platinum electrodes, Faraday Discussions, 210 (2018) 301-315.
[49] J. Souza-Garcia, C.A. Angelucci, V. Climent, J.M. Feliu, Electrochemical features of Pt(S)[n(110) × (100)] surfaces in acidic media, Electrochemistry Communications, 34 (2013) 291-294.
[50] C.E. Wartnaby, A. Stuck, Y.Y. Yeo, D.A. King, Microcalorimetric Heats of Adsorption for CO, NO, and Oxygen on Pt{110}, The Journal of Physical Chemistry, 100 (1996) 12483-12488.
[51] G. Ertl, P.R. Norton, J. Rüstig, Kinetic Oscillations in the Platinum-Catalyzed Oxidation of Co, Physical Review Letters, 49 (1982) 177-180.
[52] M. Eiswirth, G. Ertl, Forced oscillations of a self-oscillating surface reaction, Physical Review Letters, 60 (1988) 1526-1529.
[53] M. Eiswirth, G. Ertl, Kinetic oscillations in the catalytic CO oxidation on a Pt(110) surface, Surface Science, 177 (1986) 90-100.
[54] F.J. Vidal-Iglesias, N. García-Aráez, V. Montiel, J.M. Feliu, A. Aldaz, Selective electrocatalysis of ammonia oxidation on Pt(100) sites in alkaline medium, Electrochemistry Communications, 5 (2003) 22-26.
[55] F.J. Vidal-Iglesias, J. Solla-Gullón, P. Rodríguez, E. Herrero, V. Montiel, J.M. Feliu, A. Aldaz, Shape-dependent electrocatalysis: Ammonia oxidation on platinum nanoparticles with preferential (100) surfaces, Electrochemistry Communications, 6 (2004) 1080-1084.
[56] J. Solla-Gullón, F.J. Vidal-Iglesias, P. Rodríguez, E. Herrero, J.M. Feliu, J. Clavilier, A. Aldaz, In situ surface characterization of preferentially oriented platinum nanoparticles by using electrochemical structure sensitive adsorption reactions, Journal of Physical Chemistry B, 108 (2004) 13573-13575.
[57] A. Rodes, R. Gómez, J.M. Pérez, J.M. Feliu, A. Aldaz, On the voltammetric and spectroscopic characterisation of nitric oxide adlayers formed from nitrous acid on Pt{hkl} and Rh{hkl} electrodes, Electrochimica Acta, 41 (1996) 729.
[58] G.A. Attard and A. Ahmadi, Anion—surface interactions Part 3. N2O reduction as a chemical probe of the local potential of zero total charge, Journal of Electroanalytical Chemistry, 389 (1995) 175.
[59] Ricardo Martínez-Hincapié , V. Climent, J.M. Feliu Peroxodisulfate reduction as a probe to interfacial charge, Electrochemistry Communications 88 (2018) 43.
[60] ValentínBriega-Martos, EnriqueHerrero, Juan M.Feliu, Pt(hkl) surface charge and reactivity, Current Opinion in Electrochemistry, 17 (2019) 97.
[61] Matteo Duca, Marta C. Figueiredo, Victor Climent, Paramaconi Rodriguez, Juan M. Feliu, and Marc T. M. Koper, Selective catalytic reduction at quasi-perfect Pt(100) Domains: a universal low-temperature pathway from nitrite to N2, Journal of the American Chemical Society, 133 (2011) 10928.
[62] R. Martínez-Hincapié, V. Climent, J. M. Feliu, Peroxodisulfate reduction on platinum stepped surfaces vicinal to the (110) and (100) poles, Journal of Electroanalytical Chemistry, 847 (2019) 113226.
[63] A. Ahmadi, E. Bracey, R.W. Evans and G.A. Attard, Anion—surface interactions Part 2. Nitrous oxide reduction as a probe of anion adsorption on transition metal surfaces, Journal of Electroanalytical Chemistry, 350 (1993) 297.
[64] W.A. Brown, R.K. Sharma and D.A. King, Site switching and surface restructuring induced by NO adsorption on Pt{110}, Journal of Physical Chemistry B, 102 (1998) 5303.
[65] Ruben Rizo, Enrique Herrero and Juan M. Feliu, Oxygen reduction reaction on stepped platinum surfaces in alkaline media, Physical Chemistry Chemical Physics, 15 (2013) 15416.

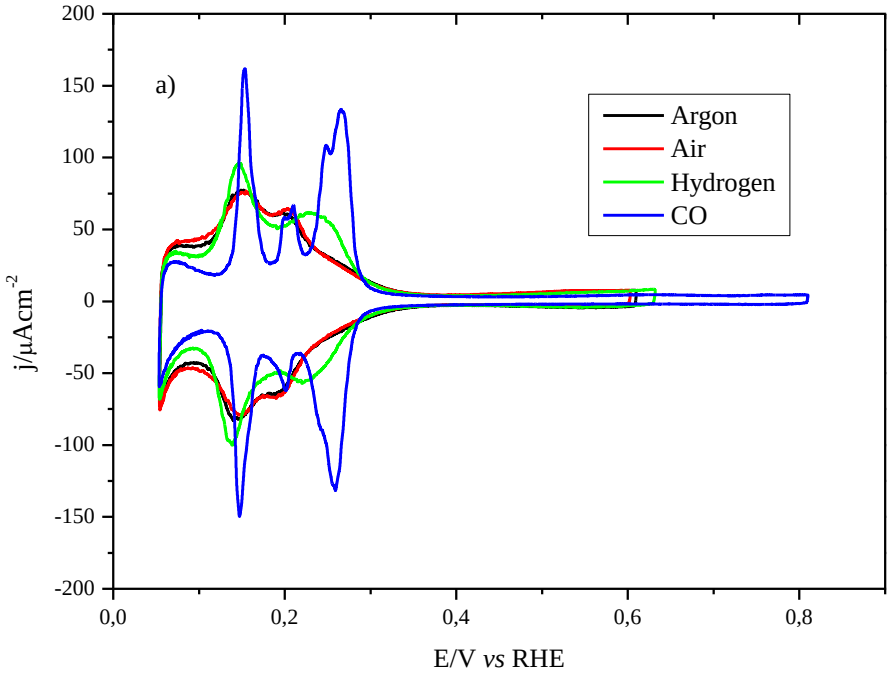
a)
Argon
Air
Hydrogen
CO
j/µAcm-2
E/V vs RHE
200
150
100
50
0
-50
-100
-150
-200
0,0
0,2
0,4
0,6
0,8

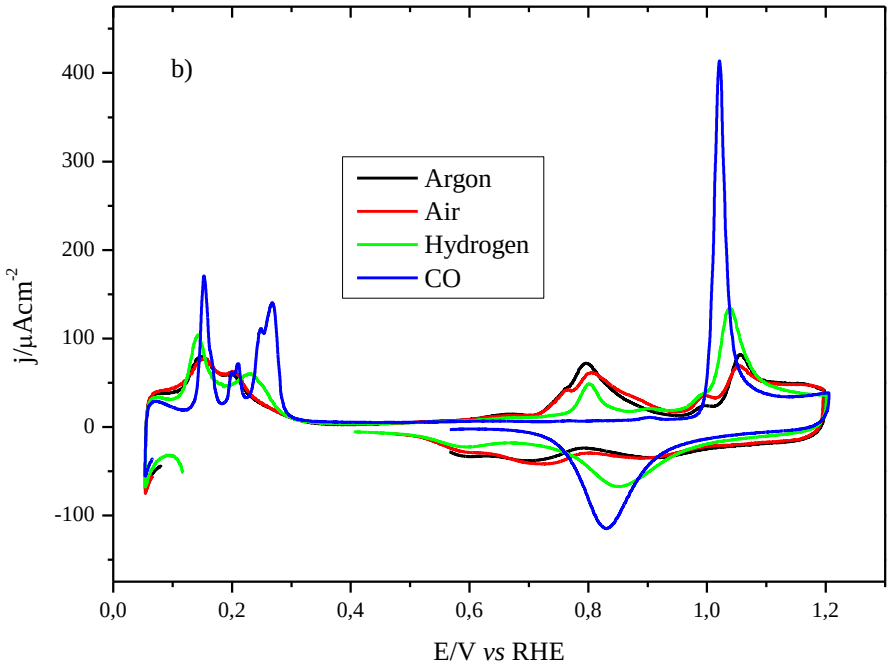
b)
Argon
Air
Hydrogen
CO
j/µAcm-2
E/V vs RHE
400
300
200
100
0
-100
0,0
0,2
0,4
0,6
0,8
1,0
1,2

Figure 1: (a) Stable CV responses of Pt{110} in 0.1 M perchloric acid cooled in different gaseous environments after flame annealing. (b) Subsequent potential cycle from 0 to 1.2 V demonstrating variations in electrochemical oxide formation depending on surface preparation. Sweep rate = 50 mV/s.

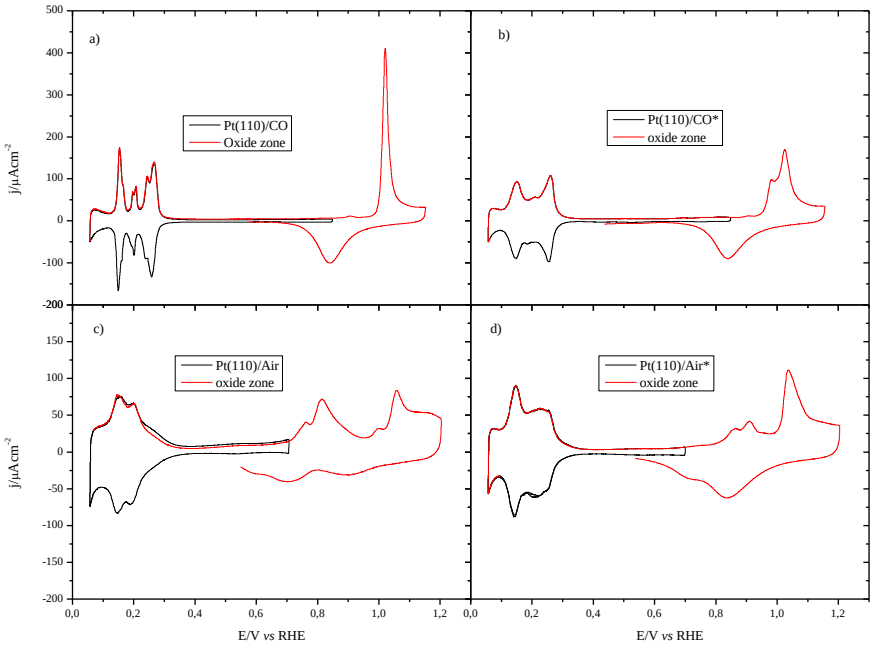

Figure 2: Stable CV responses of Pt{110} in 0.1 M perchloric acid cooled in different gaseous environments after flame annealing. Black curve corresponds to stable CV collected prior to excursion to oxide electrosorption potential region, red curve shows subsequent oxide electrosorption potential sweep. (a) Cooled in CO. (b) After first excursion into oxide region in (a). (c) Cooled in air. (d) Air-cooled electrode treated with 10 potential cycles in a solution saturated with CO. Sweep rate = 50 mV/s.

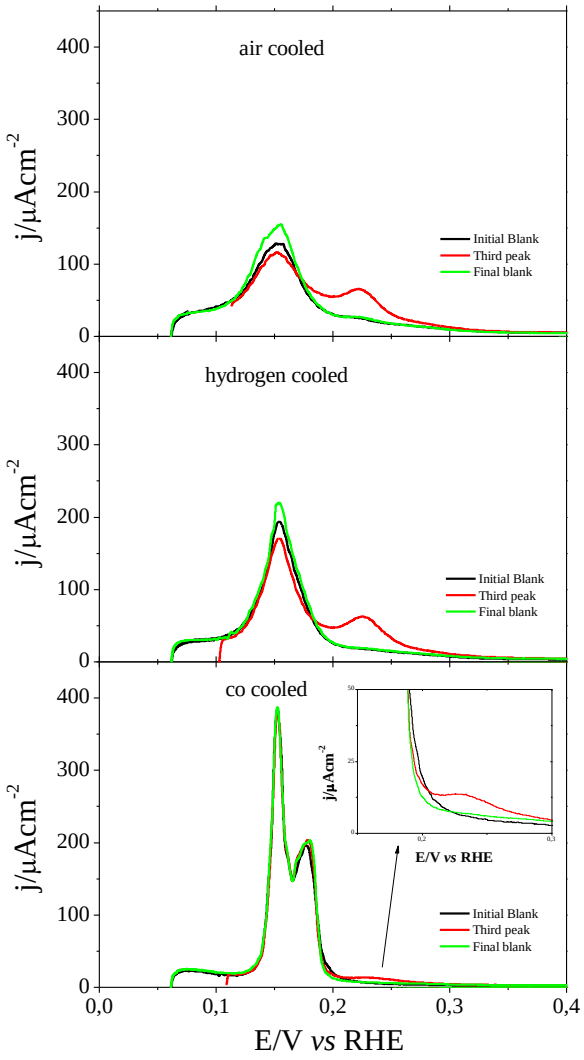

Figure 3. Third peak on Pt(110) cooled in air, hydrogen and CO. 2 minutes @ 0.02 V. 0.1 M H_2SO_4. Scan rate 50 mVs^{-1}.

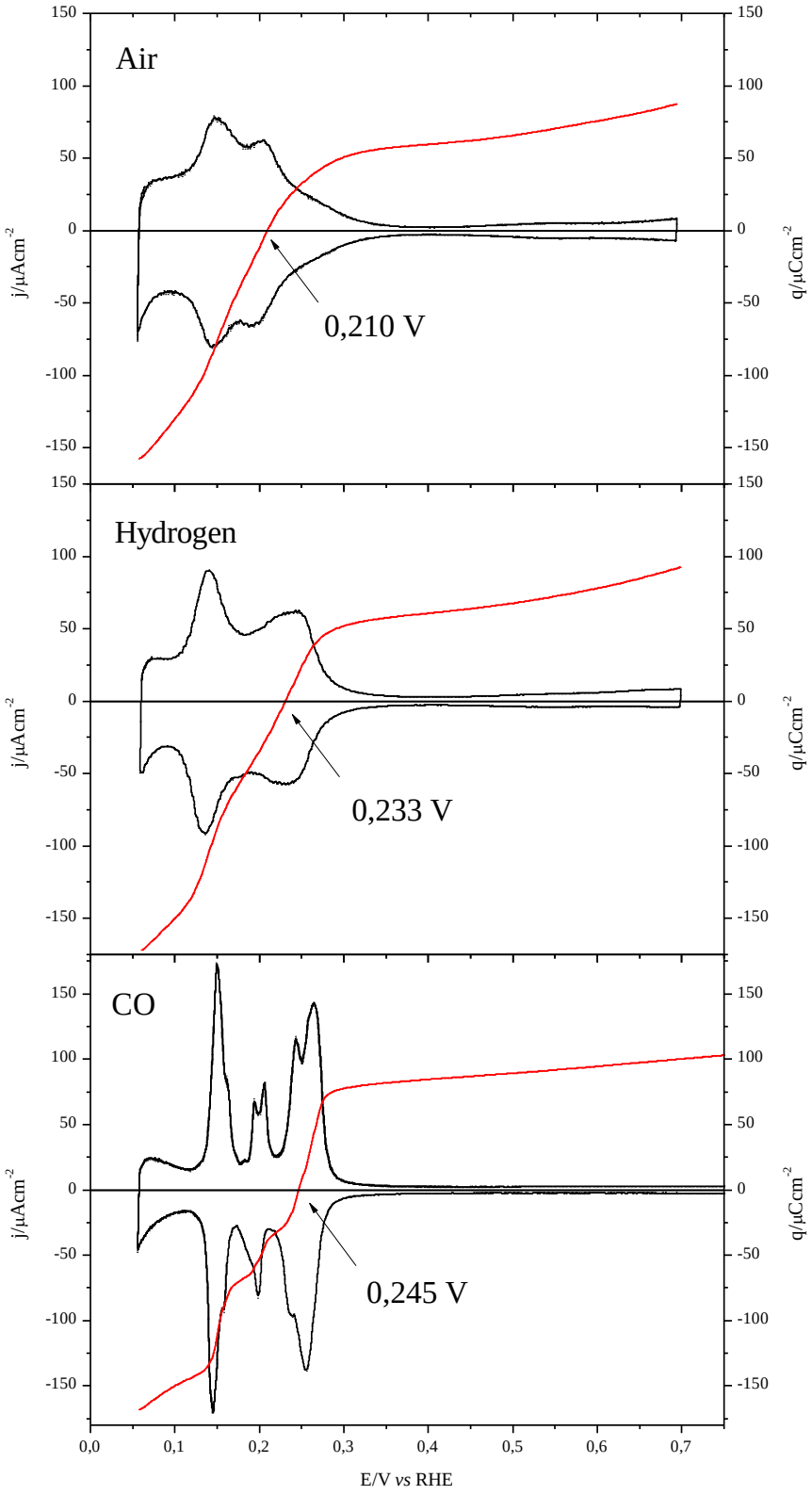

Figure 4: CO-charge displacement data for air-, hydrogen- and CO-cooled Pt{110} electrodes including values of PZTC indicated by the arrow.

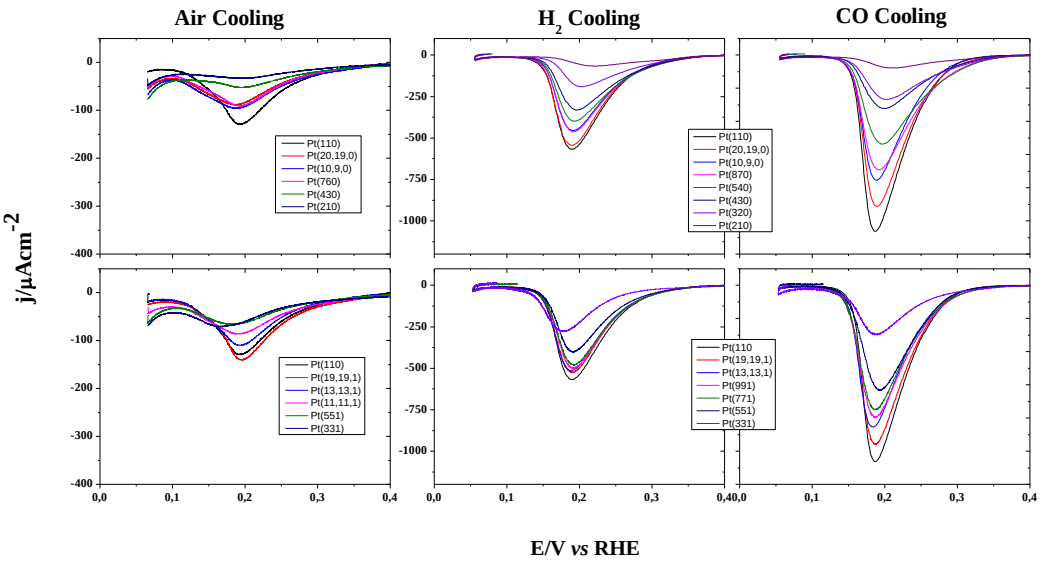

Figure 5: Nitrate reduction CVs on stepped Pt{110} electrodes in aqueous 0.1 M perchloric acid + 0.01M M KNO_3 for CO-cooled (right column), hydrogen-cooled (central column) and air-cooled (left column) electrodes. Bottom figures = Pt(S)-[nPt{110}x{111}] data, Top figures = Pt(S)-[nPt{110}x{100}] data. Sweep rate = 10 mV/s.

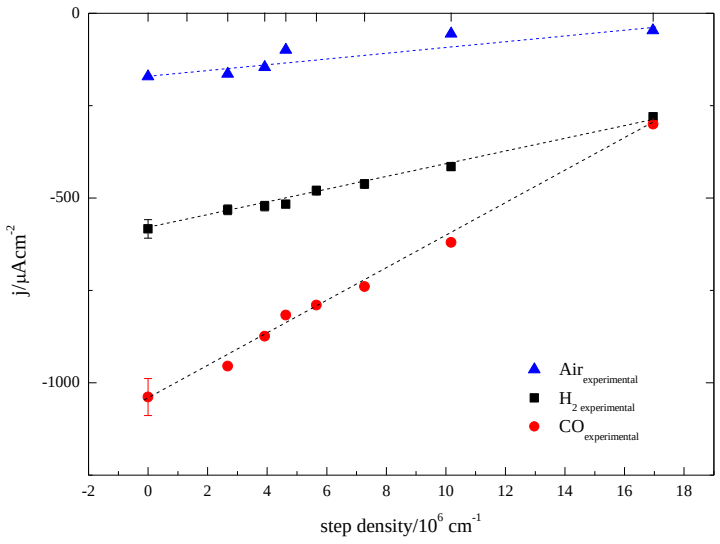

Figure 6: Plot of nitrate reduction current density versus step density for Pt(S)-[n{110}x{111}] electrodes, flame-annealed and cooled in air, hydrogen and carbon monoxide.

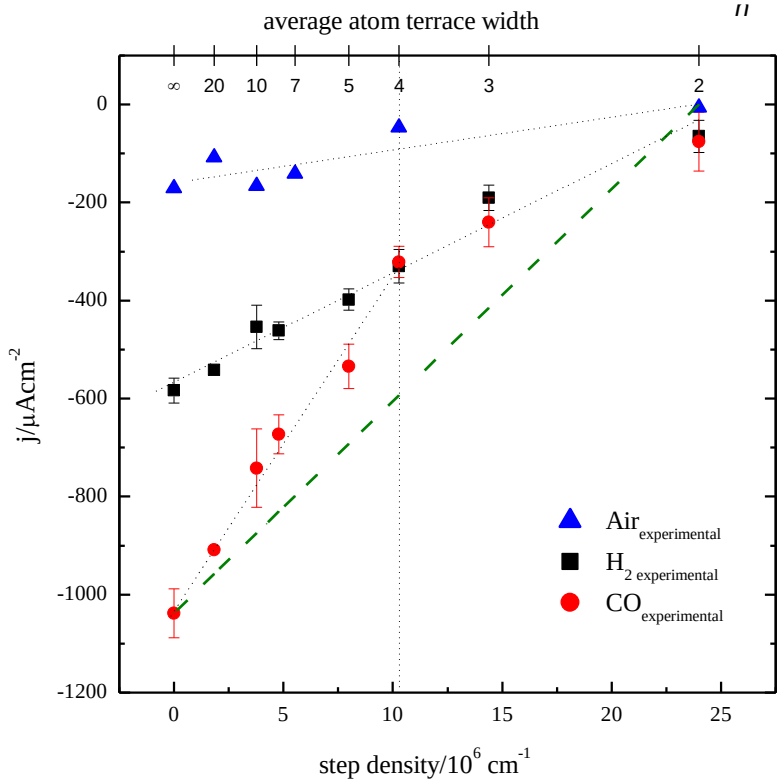

Figure 7: Plot of nitrate reduction current density versus step density for Pt(S)-[n{110}x{100}] electrodes, flame-annealed and cooled in air, hydrogen and carbon monoxide. The heavy dashed line in green indicates the theoretical behaviour if there was a one-to-one correspondence (no faceting) between "{100}" step density and nitrate reduction current density.